The Effect of Genetically Expressed Cardiac Titin Fragments on in Vitro Actin Motility

Quanning Li,* Jian-Ping Jin,‡ and Henk L. Granzier*

*Department of Veterinary and Comparative Anatomy, Pharmacology, and Physiology, Washington State University, Pullman, WA 99164-6520 USA; and ‡Department of Medical Biochemistry, University of Calgary, Calgary, Alberta, T2N 4N1, Canada

ABSTRACT Titin is a striated muscle-specific giant protein (M_r ~3,000,000) that consists predominantly of two classes of ~100 amino acid motifs, class I and class II, that repeat along the molecule. Titin is found inside the sarcomere, in close proximity to both actin and myosin filaments. Several biochemical studies have found that titin interacts with myosin and actin. In the present work we investigated whether this biochemical interaction is functionally significant by studying the effect of titin on actomyosin interaction in an in vitro motility assay where fluorescently labeled actin filaments are sliding on top of a lawn of myosin molecules. We used genetically expressed titin fragments containing either a single class I motif (Ti I), a single class II motif (Ti II), or the two motifs linked together (Ti I-II). Neither Ti I nor Ti II alone affected actin-filament sliding on either myosin, heavy meromyosin, or myosin subfragment-1. In contrast, the linked fragment (Ti I-II) strongly inhibited actin sliding. Ti I-II-induced inhibition was observed with full-length myosin, heavy meromyosin, and myosin subfragment-1. The degree of inhibition was largest with myosin subfragment-1, intermediate with heavy meromyosin, and smallest with myosin. In vitro binding assays and electrophoretic analyses revealed that the inhibition is most likely caused by interaction between the actin filament and the titin I-II fragment. The physiological relevance of the novel finding of motility inhibition by titin fragments is discussed.

INTRODUCTION

Titin (also known as connectin) is a striated muscle-specific giant protein (M_r ~3,000,000) that makes up ~10% of the myofibrillar protein mass (for reviews see Wang, 1985; Maruyama, 1986, 1994; Fulton and Issaacs, 1991; Trinick, 1991). Titin is localized inside the sarcomere, and a single molecule spans from the Z-line to the M-line region, a distance that is typically ~1–2 μm. The molecular organization of titin has been shown by cDNA cloning and sequencing to be modular. Two classes of ~100-residue motifs, class I and class II (related to fibronectin type III and immunoglobulin C2 domains, respectively) repeat along the molecule (Labeit et al., 1990, 1992; Fritz et al., 1993; Pan et al., 1994). In the A-band, the two classes of titin sequence motifs form 11 domain super-repeats (I-I-I-II-I-I-I-II-I-I-II) with a periodicity resembling the 43-nm cross-bridge repeat of the thick filament (Trinick, 1991; Labeit et al., 1992). In the I-band portion of titin the arrangement of motifs seems to be irregular, with long stretches of exclusively type II motifs (Maruyama et al., 1993; Sebestyén et al., 1995; unpublished data discussed in Politou et al., 1994).

The I-band segment of titin behaves as an elastic connector between the A-band and the Z-line and is likely to be largely responsible for the passive tension developed by striated muscle upon stretch (Wang et al., 1984; Horowits et al., 1986; Yoshioka, 1986; Fürst et al., 1988; Wang et al., 1991; Trombitás et al., 1991; Higuchi, 1992; Granzier and Irving, 1995). It has been suggested that passive tension developed by the I-band segment of titin is the result of the reversible unfolding of type II motifs (Soteriou et al., 1993a; Erickson, 1994).

The function of the A-band segment of titin, which constitutes 60–80% of the whole molecule, remains elusive. It is unlikely that this portion of the molecule plays a role in the development of passive tension because the strain of the A-band segment of titin is not altered when sarcomeres undergo physiological changes in length (Wang et al., 1984; Fürst et al., 1988; Trombitás and Pollack, 1993). This constant strain is most likely attributable to binding between titin and the thick filament because A-band titin does behave elastically after myosin extraction (Higuchi et al., 1992; Wang et al., 1993). A-band titin has been postulated to possess several other functions (Wang, 1985; Whiting et al., 1989; Labeit et al., 1992; Maruyama, 1994): it might regulate thick-filament assembly and length, and it might modulate cross-bridge interaction with actin. Because of its proximity to both myosin and actin in the A-band, titin could indeed influence actomyosin interaction. Alternatively, actin and myosin may modulate the properties of titin. Biochemical studies have shown that both native titin and cloned titin motifs interact with myosin and with actin (Kimura et al., 1984; Maruyama et al., 1987; Labeit et al., 1992; Soteriou et al., 1993b; Koretz et al., 1993; Jin, 1995). In the present work we investigated whether this biochemical interaction is functionally significant by studying the effect of titin on actomyosin interaction in an in vitro motility assay. In this model system, actin and myosin interact and produce movement and force similar to that produced by stimulated muscle (Kishino and Yanagida,

Received for publication 6 April 1995 and in final form 20 July 1995.

Address reprint requests to Dr. Henk Granzier, Department of Veterinary and Comparative Anatomy, Pharmacology, and Physiology, 205 Wegner Hall, Washington State University, Pullman, WA 99164-6520. Tel.: 509-335-3390; Fax: 509-335-4650; E-mail: granzier@unicorn.it.wsu.edu.

0006-3495/95/10/1508/11 $2.00

1988; Finer et al., 1994). Single actin filaments were visualized and their speed of sliding on top of a coverslip coated with myosin molecules was measured in the absence and presence of cloned titin fragments. Unlike muscle, the in vitro motility assay uses only proteins that are essential for muscle shortening and force generation (actin and myosin), allowing us to test directly whether titin plays a role in these important physiological processes.

We opted for using genetically expressed titin fragments of known amino acid sequence, instead of the native protein, because it is difficult to purify native titin and to prevent its degradation into fragments that are not well defined (Wang, 1985). Three different types of cloned rat cardiac titin fragments were used; they contained either a single class I motif (Ti I), a single class II motif (Ti II), or the two motifs linked together (Ti I-II). (For further information, see Jin, 1995.) Neither Ti I nor Ti II alone was found to affect actin-filament sliding. In contrast, the linked fragment (Ti I-II) strongly inhibited actin sliding. We present evidence that motility inhibition is most likely caused by interaction between the actin filament and the titin I-II fragment, and we discuss the physiological relevance of our findings.

MATERIALS AND METHODS

Protein Preparation

Titin fragments

Three cloned rat cardiac titin fragments were used. These fragments consisted of a type I sequence motif (Ti I), a type II sequence motif (Ti II), or these two motifs linked together (Ti I-II). The molecular cloning, bacterial expression, purification, and characterization of these three fragments are described in Jin (1995). The concentrations of stock solutions of purified fragments were determined by amino acid analysis (Protein Sequencing Facility, University of Calgary). The cDNA-deduced protein sequence of Ti I-II is shown in Fig. 1, and chemical properties of the protein fragments are summarized in Table 1.

Myosin

Skeletal muscle myosin was prepared from leg muscles of adult rats (male Sprague-Dawley, 8–12 weeks old) following the procedures of Yamashita et al. (1994), with minor modifications. Briefly, muscles were excised from anesthetized rats and washed with ice-cold buffered saline (10 mM sodium phosphate buffer, 150 mM NaCl, pH 7.2). Muscles were minced and then blended (model TCM-1, Tekmar Co., Cincinatti, OH) for 30 s in Tris-maleic acid buffer (20 mM Tris(hydroxymethyl)aminomethane maleic acid, 1 mM EDTA, pH 7.0), followed by centrifugation at 1000 *g* for 15 min (L5–50, Beckman, Fullerton, CA). The pellet was suspended in three volumes of a high-salt solution (100 mM KH_2PO_4, 50 mM K_2HPO_4, 0.3 M KCl, 1 mM ATP, 5 mM dithiothreitol (DTT), 5 μg/ml leupeptin, 1 mM EDTA, pH 6.5) for 7.5 min and centrifuged at 11,000 *g* for 15 min. The supernatant was collected, and 14 volumes of distilled water was added to precipitate myosin. After incubating on ice for 1 h, myosin was collected by centrifugation at 11,000 *g* for 15 min. The pellet was suspended for 10 min in a high-salt solution (0.6 M KCl, 10 mM Tris-HCl, 5 μg/ml leupeptin, 5 mM DTT, pH 7.5). The suspension was then centrifuged at 120,000 *g* for 4 h to remove trace amounts of actin. Myosin was stored on ice and used within 3 days.

MSAPATVPDPPENVKWRDRTANSIFLTWDPPKNDGGSRIKGYIVEKCPRGSDKW
VACGEPVPDTKMEVTGLEEGKWYAYRVKALNRQGASKPSKPTEEIQAVDTQEA
PEIFLDVKLLAGLTVKAGTKIELPATVTGKPEPKITWTKADTLLRPDQRITIENVP
KKSTVTITDSKRSDTGTYIIEAVNVCGRATAVVEVNVLDKPGPP

FIGURE 1 The cDNA-deduced protein sequence of Ti I-II. The sequence that corresponds to that of the Ti I fragment is underlined. The remaining sequence is that of the Ti II fragment.

TABLE 1 Deduced properties of cloned cardiac titin fragment (Jin, 1995)

Fragment	Motif	Number of residues	M_r	pI	β-sheet content (%)
Ti I	I	108	11,972	6.64	59
Ti II	II	102	10,954	9.35	34
Ti I-II	I-II	207	22,609	8.45	46

Heavy meromyosin (HMM) and myosin subfragment-1 (S-1)

HMM and S-1 were prepared from myosin following the methods described by Kron et. al (1991), with minor modifications. In brief, myosin stock was diluted with nine volumes of solution 1 (0.1 mM $NaHCO_3$, 0.1 mM EGTA, and 1 mM DTT), left on ice for 15 min, and centrifuged at 27,000 *g* for 10 min. For HMM preparation, the pellet was dissolved in an equal volume of solution 2 (20 mM imidazole-HCl, 1 M KCl, 4 mM $MgCl_2$, and 10 mM DTT, pH 7.4). After a 10-min incubation at 25°C, α-chymotrypsin (C-3142; Sigma, St. Louis, MO) was added to the solution to a final concentration of 12.5 μg/ml. After incubating for 10 min at 25°C, the solution was diluted with nine volumes of solution 1 with 3 mM $MgCl_2$ and 0.1 mM phenylmethylsulfonyl fluoride and kept on ice for 1 h. The suspension was centrifuged at 230,000 *g* for 45 min. The supernatant containing HMM was collected, stored on ice, and used within 5 days.

For S-1 preparation, the myosin pellet was dissolved in an equal volume of solution 1 with 1.2 M KCl and 20 mM DTT. After a 10-min incubation at 25°C, 19 volumes of solution 1 was added to the suspension, which was subsequently kept on ice for 15 min and then centrifuged at 27,000 *g* for 10 min. The pellet was suspended in 25 mM imidazole-HCl, 100 mM NaCl, 5 mM $MgCl_2$, and 1 mM DTT, pH 7.4, and incubated at 25°C for 10 min. Papain (P-4762, Sigma) was then added to a final concentration of 12.5 μg/ml. After a 10-min incubation at 25°C, 1.5 volumes of ice-cold solution 1 with 10 μg/ml leupeptin and 5 mM $MgCl_2$ was added to stop the reaction. The suspension was kept on ice for 1 h and then centrifuged at 230,000 *g* for 45 min. The supernatant was collected and stored on ice and used within 5 days.

The concentration of myosin, HMM, and S-1 was estimated spectrophotometrically by using as extinction coefficient (A_{280} in cm^2/mg) 0.53, 0.60, and 0.81, respectively (Margossian and Lowey, 1982). The concentration of myosin, HMM, and S-1 used in the motility assay (see below) was 0.1 mg/ml.

Actin

Actin was prepared from longissimus dorsi muscle of the rabbit and fluorescently labeled with tetramethylrhodamine-phalloidin (R-415, Molecular Probes, Eugene, OR) following the methods described by Kron et al. (1991). Labeled actin stock was stored on ice in the dark and used in the motility assay within a few weeks.

In vitro motility assay

The methods described by Kron et al. (1991) were used with some minor modification. Briefly, the motility assay chamber was constructed from

glass coverslips (No. 0, Thomas Scientific, Swedesboro, NJ) that had been cleaned with 0.1 M KOH, rinsed with distilled H_2O and 95% ethanol, and air-dried. The coverslips were dipped in a 1% solution of nitrocellulose in amylacetate (catalog number 11210, Fullham, Latham, NY) and air-dried. A flow chamber was made by using two thin slivers cut from the coverslips as spacers between two coverslips. Myosin, HMM, or S-1 solution was added to the chamber and incubated for 90 s. The chamber was subsequently washed two times with 100 μl of a solution (30 mM KCl, 20 mM HEPES-KOH, pH 7.5, and bovine serum albumin (BSA) (A-7030, Sigma) to remove unbound protein and block the exposed nitrocellulose surface. During the initial phase of the experiments, BSA concentration was 0.5 mg/ml. Although this was sufficient to block binding of actin to the nitrocellulose surface, titin fragments were still able to bind. Therefore, the BSA concentration was varied in some experiments between 0.5 and 50 mg/ml. Unlabeled actin (0.1 mg/ml) was then added to the chamber to block the ATP-insensitive rigor heads (cf. Homsher et al., 1992), followed by washing three times with ATP-containing assay buffer (25 mM KCl, 25 mM HEPES-KOH, 6 mM $MgCl_2$, 1 mM EGTA, 2 mM ATP, and 1% 2-mercaptoethanol, pH 7.8). Fluorescently labeled actin (0.5 μg/ml) in ATP solution was then introduced into the chamber. Unbound actin was washed out (two times) with the ATP solution that now contained 3 mg/ml glucose, 0.1 mg/ml glucose oxidase, and 0.015 mg/ml catalase to inhibit photobleaching. We then added ATP solution that contained titin fragments. The concentrations of these fragments varied from 0 to 5 μM for Ti I-II and from 0 to 25 μM for Ti I or Ti II.

Sliding movement of the actin filaments was viewed with use of an inverted epifluorescence microscope (Nikon Diaphot 300, Nikon, Melville, NY) with an oil-immersion objective lens (Nikon, 60×, N.A. 1.4). Both the stage and the objective lens were temperature controlled. In most experiments the temperature was 28 ± 1°C, unless indicated otherwise. Real-time images of the actin filaments were recorded with an intensified CCD camera (ICCD-100F, Video Scope Int., Washington, DC), and averaged (two frames) with an on-line image processor (Argus-10, Hamamatsu, Bridgewater, NJ) that was also used for analog contrast enhancement. Images were stored on VHS videotape.

Videotaped images were digitized into gray-scale images at four frames/s using the built-in frame grabber of a Macintosh microcomputer (Quadra 840AV, Apple Computer, Cupertino, CA) and saved as a QuickTime Moov using the program FusionRecorder (VideoFusion Inc., Maumee, OH). The position of the leading edge of the actin filaments was determined by the user, and the sliding distance was measured by tracing the position of the actin filaments in each frame using the program ImageQuickTime, a version of the public domain program National Institutes of Health Image (v1.51, originally written by W. Rasband at the National Institutes of Health, adapted by E. Shelden, University of Connecticut to read QuickTime Moov. National Institutes of Health Image and Image QuickTime are available by anonymous FTP from zippy.nimh.nih-.gov). The velocity of sliding was obtained by dividing the traveled distance by the time. Only the period during which the filament moved continuously was used for calculation of filament velocity.

Protein binding assays

Binding between the three different titin fragments and actin and myosin, under conditions similar to those of the in vitro motility assay, were studied by using both fluorescence microscopy and gel electrophoresis.

Binding of fluorescent actin filaments to titin fragments

This binding was studied by using fluorescence microscopy. Proteins were loaded into the flow chamber used for the in vitro motility assay (see above). Three types of loading sequences were used. In the first, titin fragments were added to the flow chamber and incubated for 5 min. The chamber was washed two times with BSA solution (5 mg/ml) and incubated for 5 min with BSA. Fluorescently labeled actin filaments (2 μg/ml) were then added to the chamber and incubated for 2 min, after which the chamber was washed with BSA-containing buffer. This loading sequence was thus titin → BSA → actin. The other two loading sequences were BSA → titin → actin and BSA → actin → titin. The fluorescently labeled actin filaments were then imaged, as described above. We counted the number of actin filaments within the field of view and determined their total length.

Binding of titin fragments to BSA-coated glass surface

Gel electrophoresis was used to study whether titin fragments were able to bind to a nitrocellulose-treated glass surface after BSA blocking. Because only very small amounts of proteins can be expected to bind to the coverslip of the motility chamber, for this study we used glass capillaries that have a higher surface area to volume ratio than the motility chamber does. This allowed us to recover a larger amount of bound protein for a given volume of solubilization buffer. The inner surface of a glass micropipette (50 μl, VWR 53432–783) was cleaned and treated with nitrocellulose and was then blocked with BSA of varying concentrations (0.5–50 mg/ml) for 5 min. Titin fragments (5 μM) were then drawn into the micropipette. After a 5-min incubation, the micropipette was washed five times to remove unbound proteins. Proteins bound to the surface of the micropipette were solubilized for 45 s by drawing into the pipette 50 μl of solubilization buffer (2% sodium dodecyl sulfate (SDS), 50 mM Tris-Cl, 37 μg/ml pyronin-Y, 10% v/v glycerol, and 100 mM DTT, pH 8.0) at 100°C. The samples were subjected to electrophoresis by using Laemmli gels with 12% acrylamide and were silver-stained, according to Granzier and Wang (1993a,b,c).

Binding of titin fragments to myosin

Titin fragments (5 μM) were loaded into nitrocellulose-coated glass capillaries and incubated for 5 min. The inner surface was then blocked for 5 min with BSA (5 mg/ml) by washing the capillary two times with BSA solution, followed by a 2-min incubation with monomeric myosin (0.5 mg/ml) or HMM (0.6 mg/ml). To bring the ionic strength of the myosin-containing buffer closer to physiological but still keep myosin depolymerized, myosin was diluted just before loading into the capillary with assay buffer (see above). This lowered the ionic strength from ~620 mM to 340 mM. (Centrifugation of myosin in this solution indicated that myosin did not form filaments.) After incubating with myosin for 2 min, the capillaries were washed five times with either in vitro motility assay buffer or with this assay buffer that contained an additional 300 mM KCl. HMM-loaded capillaries were washed with only in vitro motility assay buffer. After a 5-min incubation period, proteins bound to the surface were solubilized, subjected to electrophoresis, and silver-stained as described above. Control experiments were conducted in which myosin and HMM was added to capillaries without Ti I-II and blocking (positive control) and without Ti I-II but with blocking (negative control).

Statistics

The results of our studies will be given as the mean ± SD, unless indicated otherwise. Significance in selected parameters was examined with the Student's *t*-test at $p < 0.05$

RESULTS

Effect of titin fragments on motility

When HMM and S-1 were used in the absence of titin fragments, actin filaments continued sliding for many minutes without stopping. The velocity of sliding was 7.5 ± 0.5 μm/s ($n = 52$) for HMM and 1.6 ± 0.2 μm/s ($n = 36$) for S-1. When monomeric myosin was used, sliding was occasionally interrupted by brief periods without movement. For

velocity measurements we analyzed only periods of uninterrupted sliding lasting at least 5 s. The velocity was 4.90 ± 0.6 μm/s (n = 35). These results are in general accord with those reported by others (Kron et al., 1991; Homsher et al., 1992; Sellers et al., 1993).

When titin fragments were incubated together with actin filaments before their addition to the flow chamber, large nonmotile fluorescent complexes were seen in the case of the Ti I-II fragment (results not shown). This effect was absent when Ti I and Ti II were used. Unlike Ti I and Ti II, Ti I-II seems to be able to cross-link actin filaments. Actin cross-linking was absent when Ti I-II was added after actin filaments were loaded into the chamber, and single actin filaments that were mobile could now be observed.

The effect of the three different titin fragments, Ti I, Ti II, and Ti I-II, on actin filament velocity was studied with HMM. Ti I and Ti II, at concentrations between 0 and 25 μM, did not affect sliding in a statistically significant manner, whereas Ti I-II strongly inhibited sliding (Fig. 2). Velocity was reduced by ~80% when 5 μM Ti I-II was present in the assay buffer. The motility inhibition was maintained after extensive washing with Ti I-II-free ATP-containing assay buffer. We tested whether the presence of both labeled and unlabeled actin filaments (added to block irreversible rigor heads; see Materials and Methods section) in the assay had an effect on the degree of motility inhibition and found that when only labeled actin was present, the degree of inhibition was identical (results not shown).

Ti I-II-based inhibition of actin sliding was observed not only with HMM but was also observed with monomeric full-length myosin and with S-1 (Fig. 3). The degree of inhibition was largest in the case of S-1, intermediate with HMM, and smallest with full-length myosin (Fig. 3). In the presence of 2 μM Ti I-II, inhibition of sliding was ~20% in the case of myosin, ~60% with HMM, and ~80% with S-1. Fig. 3 also shows that the shape of the relation between the velocity and the Ti I-II concentration varied with the type of motor that was used, and that with S-1 the relation most resembled a hyperbola.

The velocity of sliding as a function of actin-filament length was also measured. Sliding velocity was found to be independent of actin filament length in both the absence and the presence of Ti I-II (Fig. 4). Thus, although the average velocity decreased with increasing Ti I-II concentration, there was no correlation between velocity and filament length at a given Ti I-II concentration.

The presence of Ti I-II also resulted in fracturing of actin filaments in addition to the depression of actin sliding velocity discussed above. The average length of moving actin filaments became progressively less with increasing concentrations of Ti I-II fragment (Fig. 5). The relation between actin-filament length and Ti I-II concentration

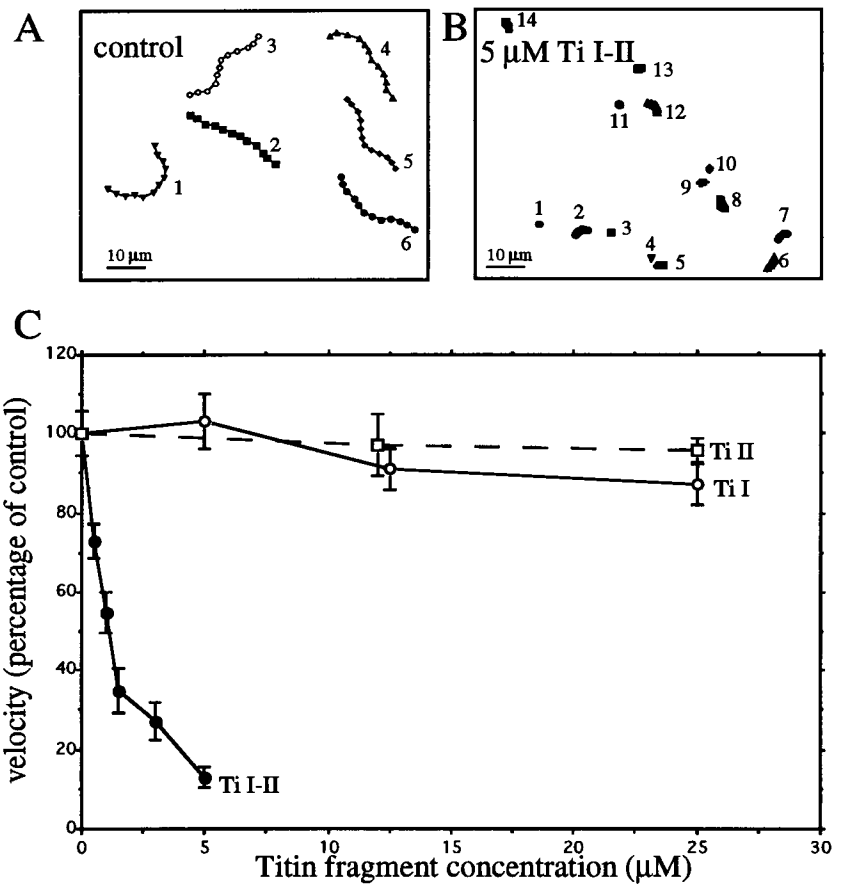

FIGURE 2 Effect of Ti I, Ti II, and Ti I-II on the velocity of actin filaments sliding over a glass surface coated with HMM, and blocked by BSA. (*A*) and (*B*): Centroid plots. The positions of the centroid of actin filaments were determined 12 times with 0.4-s intervals. (*A*) Six different actin filaments are shown under control conditions, each filament clearly moved as indicated by the winding paths of their centroids. (*B*) Motility occurred in the presence of 5 μM Ti I-II. The centroids of 14 different filaments are shown. Filaments were much less motile than under control conditions. (*C*) Effect of titin fragments on actin sliding velocity. Ti I and Ti II did not affect sliding, whereas Ti I-II inhibited sliding velocity. The velocity was measured ~2 min after the addition of Ti I-II (n for each data point is ~50.)

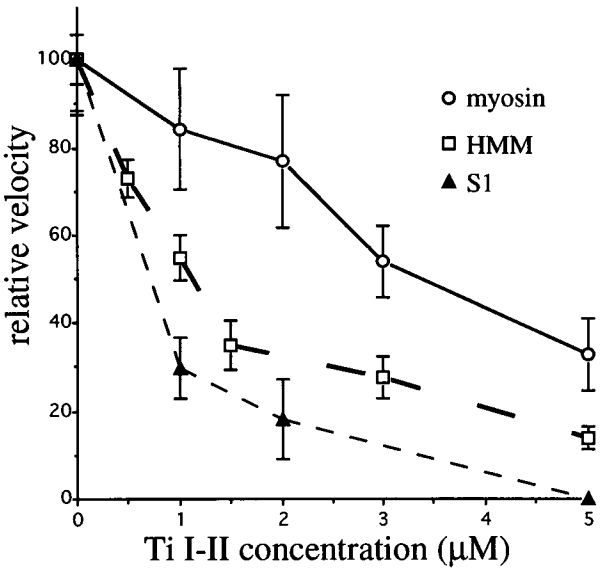

FIGURE 3 Relative velocity as a function of Ti I-II concentration; results obtained with myosin, HMM, and S1. Relative velocity decreased with increasing Ti I-II concentration, and the decrease was largest with S-1, intermediate with HMM, and smallest with myosin. (Only motile filaments were analyzed.) (n is ~50.)

seemed biphasic, with an initial steep length decrease at concentrations between 0 and 1.5 μM Ti I-II and only a modest additional decrease at higher concentrations (Fig. 5).

The presence of Ti I-II fragments also resulted in the appearance of nonmotile actin filaments. Fig. 6 shows that the percentage of filaments that moved within the period of observation was constant under control conditions but decreased dramatically within several minutes after the addition of 5 μM Ti I-II. We computed the average fraction of filaments within the field of view that was moving (as explained in Fig. 7) at a range of Ti I-II concentrations and found that the fraction decreased from >95% under control conditions to <25% in the presence of 5 μM Ti I-II (Fig. 7). The decrease was steep between 0 and 1.5 μM and more modest at higher Ti I-II concentrations (Fig. 7).

Binding of fluorescent actin filaments to titin fragments

To investigate the mechanism of the inhibitory effect of Ti I-II on actin sliding, we studied the possible interaction between Ti I-II and actin by using an in vitro binding assay that allowed us to detect binding visually. Nitrocellulose-treated coverslips were incubated with titin fragments, followed by blocking of the surface with BSA. Subsequently, fluorescent actin filaments were added, and the flow-cell was washed extensively. Interestingly, a large number of actin filaments were found (Fig. 8A) attached along their full length to the coverslip, as indicated by the complete absence of Brownian motion. To test whether actin bound to Ti I-II, or perhaps to BSA, actin was added to the flow chamber after it was coated with only BSA, without the prior addition of titin fragments, and the flow chamber was then extensively washed. No actin filaments were seen attached to the coverslip (Fig. 8 *B*). Thus, actin filaments seemed to bind to Ti I-II, resulting in the immobilization of actin filaments on the surface of the coverslip. When Ti I-II was replaced by Ti I or Ti II, no actin immobilization was observed. To test whether these two fragments were able to tether actin filaments to a surface that did not contain BSA, actin was added immediately after coating the coverslip with Ti I or Ti II, omitting the BSA step. No actin binding was observed.

To test whether Ti I-II can bind actin filaments to the surface of coverslips that are coated with BSA before the addition of Ti I-II, we first blocked the nitrocellulose-coated coverslips with BSA and then added either titin followed by actin (Fig. 8 *C*) or actin followed by washing in titin (Fig. 8 *D*). Note that the latter loading sequence was similar to the one used in the motility assay. In both cases it was found that actin filaments were still able to bind to the coverslip (Fig. 8, *C* and *D*). This indicates that despite BSA blocking, Ti I-II is still able to bind to both the coverslip and the actin filaments.

Binding of titin fragments to a BSA-coated glass surface

We tested whether Ti I-II is able to bind to a nitrocellulose-coated glass surface after BSA blocking by analyzing the proteins bound to glass capillaries with use of gel electrophoresis. The capillaries were loaded with a range of BSA concentrations (5–50 mg/ml), washed, and then incubated with Ti I-II. After extensive washing, hot solubilization buffer was loaded in the capillary, and the solubilized proteins were subjected to electrophoresis. Fig. 9 shows that after blocking with BSA, Ti I-II was still able to bind to the surface of the capillary. The amount of bound Ti I-II did drop when the BSA concentration was increased, but there was still a substantial amount bound at the highest BSA concentration tested (50 mg/ml). These results confirm our earlier finding that Ti I-II binds to the nitrocellulose-coated glass surface, even if this surface is coated first with BSA.

Binding of titin fragments to myosin

We tested binding between Ti I-II and myosin using SDS-polyacrylamide gel electrophoresis. Ti I and Ti II were not studied because they did not inhibit motility. Glass capillaries were coated with Ti I-II (5 μM) and blocked with BSA, followed by the addition of either monomeric myosin or HMM and extensive washing. Control experiments consisted of incubating myosin or HMM in capillaries that had not been treated with Ti I-II and that were not blocked (positive controls). Large amounts of myosin and HMM were bound to the surface (Fig. 10, lanes 1 and 5). When Ti I-II was omitted but the capillary had been blocked with

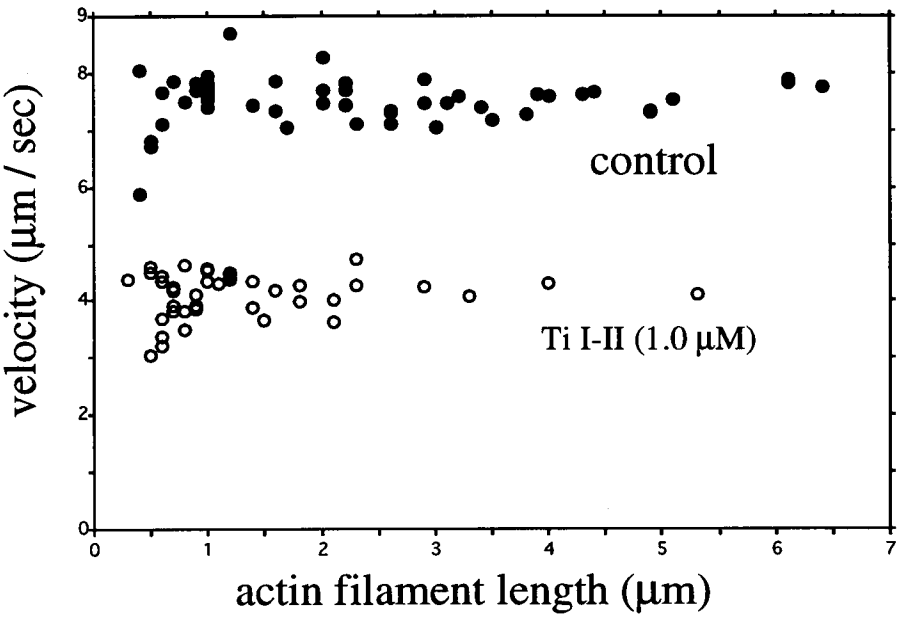

FIGURE 4 Sliding velocity of actin filaments as a function of filament length in the absence (control) and in the presence of Ti I-II (1.0 μM). Although the average speed was much less in the presence of Ti I-II than in the control, sliding speed in both cases was independent of filament length. HMM was used as motor in these experiments.

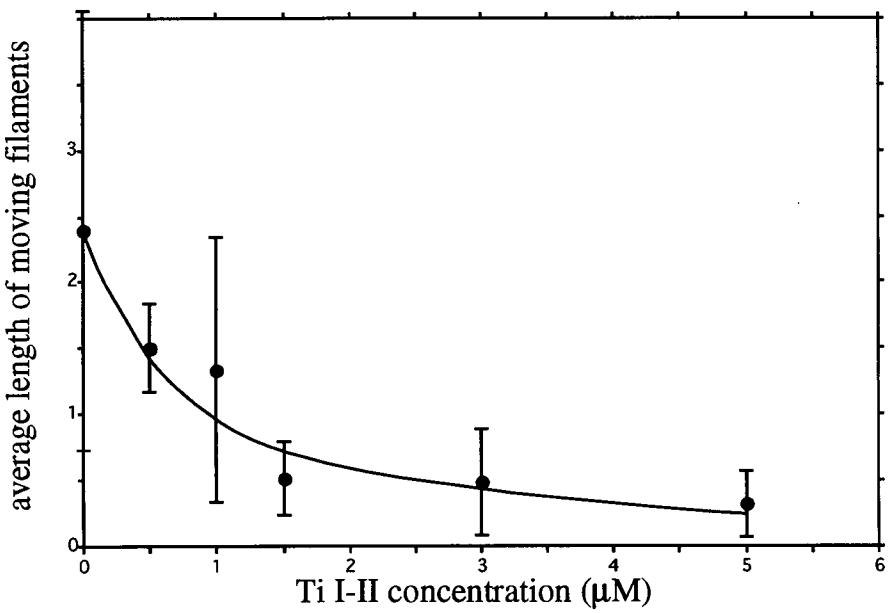

FIGURE 5 Decrease in average length of sliding actin filaments in the presence of various Ti I-II concentrations. The average length progressively decreased with increasing Ti I-II concentration. The length decreased steeply in the concentration range from 0 to 1.5 μM and then became much more shallow. HMM was used as motor. (n was typically > 30.)

BSA before loading of myosin or HMM (negative control), only very small amounts of myosin and HMM bound to the capillaries (Fig. 10, lanes 2 and 6), indicating that nonspecific binding was very low. Finally, the capillaries were coated with Ti I-II, blocked with BSA, incubated with myosin or HMM, and then extensively washed. Myosin was present in the in vitro motility assay buffer that contained an additional 300 mM KCl and was washed either with the same solution or with only assay buffer. In both cases a large amount of myosin was bound to the capillary (Fig. 10, lanes 3 and 4). Thus myosin binds to Ti I-II under in vitro motility conditions and under conditions of elevated ionic strength. When capillaries were incubated with HMM followed by washing with assay buffer, HMM binding was negligible (Fig. 10, lane 7). Thus, in contrast to myosin, HMM does not bind to Ti I-II.

DISCUSSION

The effect of three cloned titin fragments on in vitro motility of actin was studied. Ti I and Ti II, which contain a single class I and a single class II sequence motif, respectively, did not affect motility. In contrast, fragment Ti I-II, which contains a class I motif linked to a class II motif, strongly inhibited motility. Inhibition was largest when S-1 drove

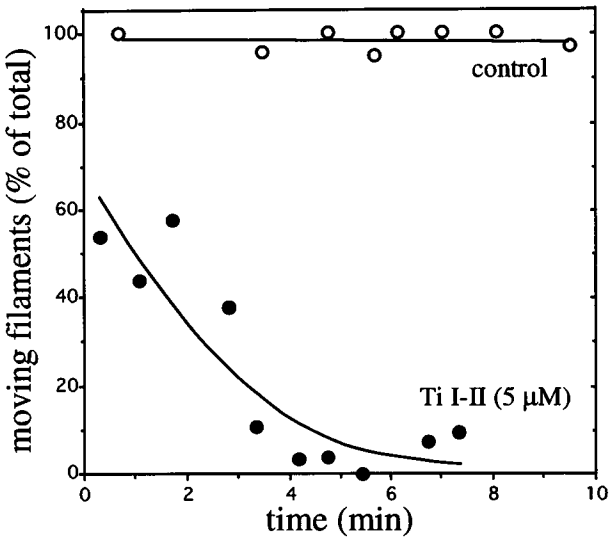

FIGURE 6 Time course of Ti I-II effect on the percentage of motile filaments. The percentage dropped quickly after the addition of 5 μM Ti I-II and reached a steady low value within 4 min. (HMM was used as motor.) (Only mean values are shown.)

motility, intermediate with HMM, and smallest with myosin. Below we discuss the possible mechanisms that underlie this inhibition and their possible relevance to muscle physiology.

Binding properties of titin fragments

We found that Ti I-II binds to a nitrocellulose-coated glass surface that had been blocked with BSA (Fig. 9). Because the amount of Ti I-II that binds to the surface decreases when the amount of bound BSA increases (Fig. 9), it is likely that Ti I-II binds to the nitrocellulose and not to the BSA. Even after blocking with BSA at a concentration of 50 mg/ml, which is 100-fold higher than normally used in the in vitro motility assay (Kron et al., 1991), a considerable amount of Ti I-II still binds to the surface (Fig. 9). Apparently, blocking with BSA does not completely abolish the binding of proteins to the nitrocellulose. Conceivably, the layer of BSA molecules attached to the coverslip has small gaps that allow a small and slender protein, such as Ti I-II, to bind to the nitrocellulose.

Ti I-II also binds to actin and tethers actin filaments to the surface of the motility chamber (Fig. 8), a phenomenon that is absent when Ti I or Ti II is used. It is possible that tethering of actin filaments requires fragments of a minimal length, and that Ti I and Ti II are too short. This possibility will be addressed in future work using fragments that contain two class I or two class II motifs. On the other hand, absence of tethering by Ti I and Ti II may result from their much lower binding affinity for F-actin than was observed both in solid-phase binding assays and in F-actin co-sedimentation assays (Jin, 1995), assays in which length effects do not play a role. Our findings are consistent with the proposal that linking a type I and type II motif greatly enhances the F-actin binding affinity beyond that of the individual motifs (Jin, 1995). The exact nature of the interaction between Ti I-II and actin remains to be established, although it is unlikely that it is purely a nonspecific electrostatic interaction, because the pI of Ti I-II is intermediate between that of Ti I and Ti II (Table 1), and neither Ti I nor Ti II binds to F-actin in the in vitro motility buffer.

This work showed that Ti I-II binds to myosin, in agreement with solid-phase binding assays with Ti I-II (Jin, 1995). In addition we found that Ti I-II did not bind to HMM (Fig. 10), indicating that Ti I-II binds to the LMM part of the myosin molecule. These results are consistent with those obtained with native titin (Soteriou et al., 1993b).

It remains to be established whether different motifs of the titin molecule have binding properties similar to those used in this study. Less than half the amino acids are conserved in class I and class II motifs (Trinick, 1991), and it is likely therefore that the binding properties of different motifs belonging to the same class are not exactly the same. Our results show that the motifs that we used bind both myosin and F-actin, and it is likely that other motifs with closely resembling sequences have similar binding properties.

Ti I-II-based inhibition of actin motility

Binding between Ti I-II and actin could affect actomyosin interaction in a number of ways. For example, Ti I-II binding to actin could block myosin binding sites ("blocking mechanism"), thereby decreasing the number of myosin heads that can interact with actin, similar to the blocking of myosin binding sites that occurs when smooth muscle caldesmon binds to actin filaments (Haeberle et al., 1992). Because the sliding velocity of F-actin is independent of its length (Fig. 4, control curve), sliding is likely to be independent of the number of myosin molecules interacting with the actin filament. Thus the blocking mechanism would therefore result in filaments that are either sliding with normal speed (intermediate degree of blocking), as found with caldesmon (Haeberle et al., 1992), or that are not sliding at all (full blocking). This is clearly contrary to our findings (Figs. 2–4). Thus it is unlikely that blocking of myosin binding sites underlies the Ti I-II-induced motility inhibition.

Another actin-based mechanism to be considered is that because of the actin-binding properties of Ti I-II (Fig. 8) and the ability of the fragment to bind to BSA-coated coverslips (Fig. 9), Ti I-II tethers the actin filament to the surface of the motility chamber and thereby exerts a force that opposes actin sliding ("actin-tethering mechanism"). Such force would decrease the sliding velocity (Figs. 2 and 3) and could result in fracturing of moving filaments (Fig. 5). The finding that at a given Ti I-II concentration the sliding velocity is independent of filament length (Fig. 4) is in agreement with the actin-tethering mechanism. The total

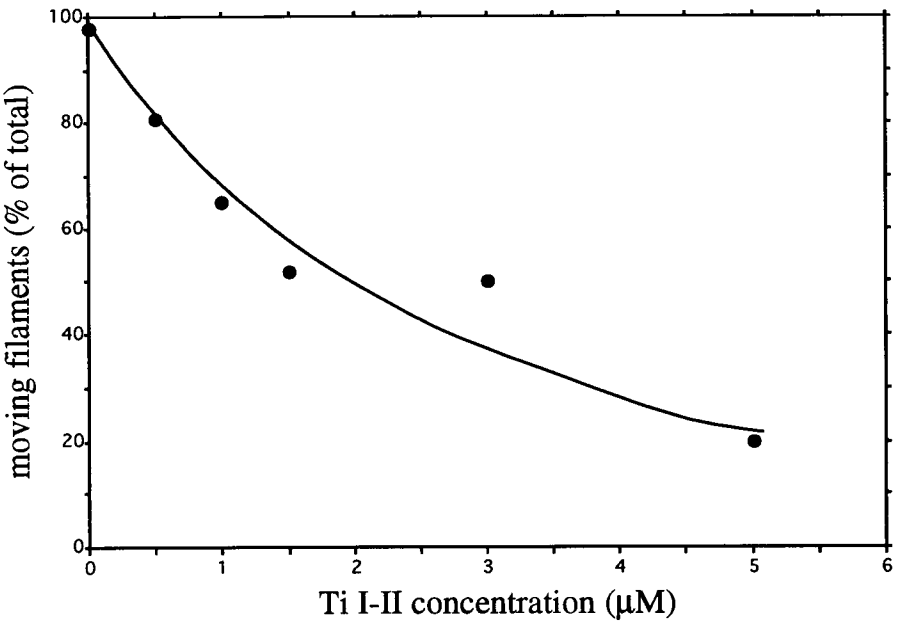

FIGURE 7 Effect of the Ti I-II concentration on the relative number of motile actin filaments. Filaments in ten different fields of view were counted within the first 8 min of observation. Two fields/min were counted for the first two min and then one field/min for the remaining time. In the absence of Ti I-II, 98% of actin filaments were moving, and this value decreased to 20% at 5 μM Ti I-II. (HMM was used as motor. The total number of filaments for each data point varied between ~200 and ~400. Only mean values are shown.)

number of Ti I-II fragments bound to actin is likely to increase linearly with actin filament length, as will be the force that opposes sliding. This is on the basis of the observation that Brownian motion is absent in all segments of the actin filaments that are bound by Ti I-II to the coverslip (as in Fig. 8 *A*), indicating that there are large numbers of Ti I-II binding sites along the actin filament. Because the number of myosin heads that interacts with actin and drives sliding also increases linearly with filament length, the force that opposes sliding is at all filament lengths predicted to be a constant proportion of the driving force. Hence sliding velocity will be less than in the control but independent of filament length, as we found in this study (Fig. 4).

The observation that inhibition of motility is highest with S-1, intermediate with HMM, and lowest with full-length myosin (Fig. 3) is also consistent with the tethering mechanism of motility inhibition. The tethering force that opposes sliding is independent of the type of motility motor that is used to drive sliding (i.e., myosin, HMM, or S-1), and the tethering force will thus be highest in proportion to the driving force when the density of mechanically active heads attached to the coverslip is the lowest. The likelihood that the myosin head is attached to nitrocellulose in a fashion allowing it to mechanically interact with actin filaments decreases when the size of the myosin subfragment is smaller (Kishino and Yanagida, 1988; Toyoshima, 1993). The density of mechanically active heads is thus likely to decrease in the order of myosin, HMM, and S-1, and the actin tethering mechanism predicts an increase in motility inhibition in the same order, as observed (Fig. 3). In a recent preliminary study we tested whether lowering the density of mechanically active myosin heads enhances motility inhibition by decreasing the HMM concentration used to load the motility chamber (from 0.5 mg/ml to 0.02 mg/ml) while keeping the Ti I-II concentration constant (1 μM). We found that lowering the HMM density did not affect the sliding velocity in the absence of Ti I-II, whereas the degree of inhibition was greatly enhanced (Kellermayer et al., in preparation), as predicted by the tethering mechanism of motility. An alternative explanation for the different sensitivity to motility inhibition of myosin, HMM, and S1 is that tethering of actin filaments by Ti I-II lifts the actin filaments from the surface by a distance that is most favorable for interaction with myosin, less favorable for HMM, and least favorable for interaction with S-1.

It is unlikely that the inhibition of motility that we observed results from Ti I-II-myosin interaction. A mechanism by which Ti I-II tethers actin filaments to myosin molecules is not likely because motility inhibition would then have to disappear when HMM is used instead of myosin, because Ti I-II binds to only myosin (Fig. 10). Instead, inhibition is more pronounced with HMM then with myosin (Fig. 3). An alternative mechanism in which a rapidly reversible interaction between Ti I-II in the solution and the myosin head depresses the myosin ATPase, which would then lead to a lower sliding velocity, is also unlikely. This conclusion is on the basis of our findings that the inhibition of motility remains after Ti I-II is washed out of the motility chamber and that the degree of inhibition increases when the density of HMM attached to the nitrocellulose decreases.

In summary, our findings do not support that the interaction between Ti I-II and myosin underlies the motility inhibition that we observed, but instead they are consistent with the actin-tethering mechanism. Our work was initiated to establish whether titin affects actomyosin interaction, and we found that the Ti I-II fragment indeed affects this interaction in the in vitro motility assay, but only indirectly by

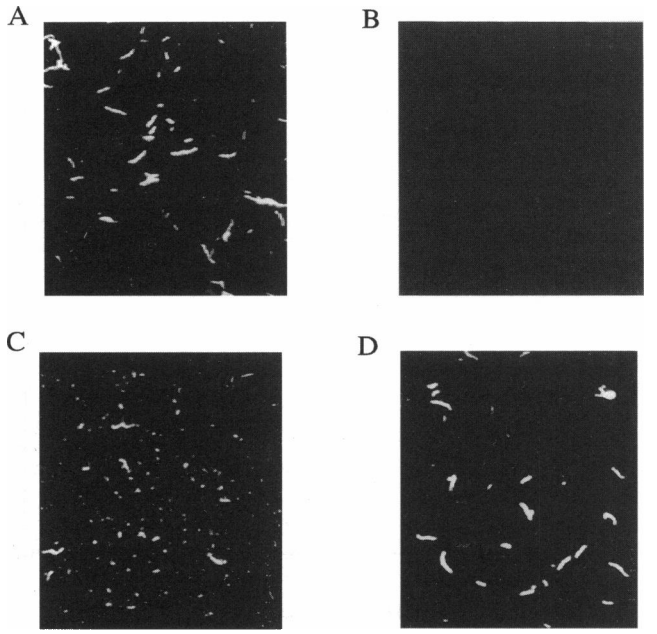

FIGURE 8 Effect of Ti I-II on the binding of fluorescently labeled actin filaments to nitrocellulose-coated coverslips. Representative images are shown. (*A*) The flow chamber was coated with Ti I-II (3 μM), and then blocked with BSA (5 mg/ml). Subsequently, actin filaments (2 μg/ml) were added and extensive washing followed. Actin filaments attached to the coverslip were observed. (*B*) The same loading sequence was used as before with the omission of Ti I-II. No actin filaments were seen. (*C*) The flow chamber was first blocked with BSA (5 mg/ml); Ti I-II (3 μM) was added, actin filaments (2.5 μg/ml sonicated actin) were added, and the flow chamber was then washed. A large number of actin filaments bound to the surface. (*D*) The flow chamber was blocked with BSA (5 mg/ml), followed by the addition of actin filaments (2 μg/ml) and Ti I-II (3 μM). Actin filaments were bound to the surface.

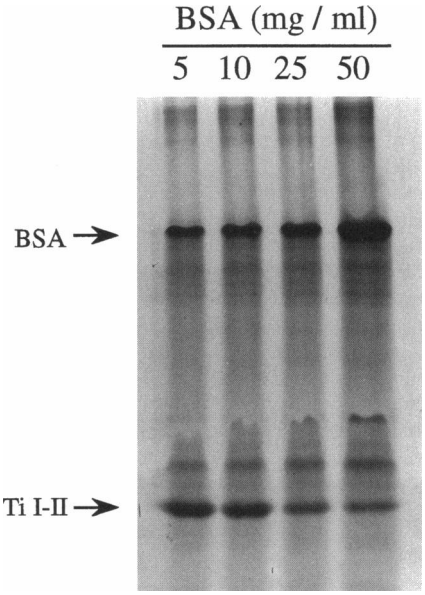

FIGURE 9 SDS-polyacrylamide gel electrophoresis analysis of Ti I-II binding to nitrocellulose-coated glass capillaries. The capillaries were blocked with BSA (5–50 mg/ml), followed by the addition of 5 μM Ti I-II and extensive washing. Proteins bound to the capillary surface were then solubilized and subjected to electrophoresis on 12% Laemmli gels. At all BSA concentrations tested, Ti I-II bound to the surface of the pipette.

tethering actin filaments and exerting a load against which actomyosin interaction has to work.

Actin-tethering mechanism

In the hypothesized actin-tethering mechanism for inhibition of in vitro actin motility, Ti I-II binds to both the nitrocellulose-coated coverslip and the actin filament, thereby inhibiting actin sliding. How Ti I-II binds to actin remains to be established. Ti I-II is likely to possess two binding sites for actin because it bundles actin filaments in solution. The locations of the two binding sites remains to be established. Because the sliding of actin filaments in the presence of Ti I-II continues for a long time at a depressed velocity, Ti I-II must continuously detach and reattach to the actin filament. Although it is not known whether the fragment unfolds before detaching from actin, we assumed that it did in order to calculate the maximum duration of attachment to actin. Assuming that the Ti I-II fragment completely unfolds before detaching from actin, increasing its length from ~8 nm to ~60 nm (Erickson, 1994), then at a sliding velocity of 4 μm/s (as in Fig. 4) Ti I-II may remain attached to actin for a maximum of ~15 ms. The attachment time will be less if the degree of Ti I-II unfolding before detachment is less than assumed. Thus the attachment time of Ti I-II to actin is on the millisecond time scale.

Physiological significance

Whether motility is inhibited by Ti I-II in a buffer with a physiological ionic strength (~180–200 mM) was not investigated because in vitro motility does not occur under such conditions (see Kron et al., 1991; Homsher et al., 1992; Sellers et al., 1993). Instead, we tested in a recent study the ionic strength dependence of the binding between Ti I-II and F-actin (using the assay explained in Fig. 8) and found binding at ionic strengths ranging from ~50-~200 mM (Kellermayer et al., in preparation). Ti I-II is thus able to tether F-actin to the surface of the motility chamber at a wide range of ionic strengths, including the physiological range, and hence Ti I-II-based inhibition of motility may indeed take place at physiological ionic strength.

There are also published reports of binding between native titin and F-actin. Using turbidimetry and flow birefringence measurements, Kimura et al. (1984) and Maruyama et al. (1987) reported evidence that native titin interacts with F-actin (ionic strength ~150 mM). Soteriou et al. (1993b) used solid-phase binding assays and reported weak binding between native titin and actin bound to nitrocellulose at an ionic strength of ~225 mM. Furthermore, a recent ultrastructural study on cardiac muscle revealed that titin and actin do not form separate filaments in the I-band; instead they make up a composite filament (Funatsu et al.,

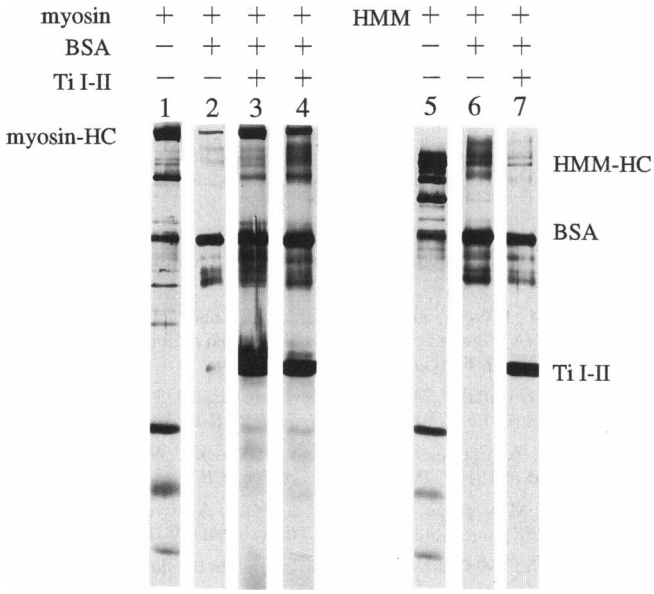

FIGURE 10 SDS-polyacrylamide gel electrophoresis analysis of Ti I-II binding to myosin and HMM. Nitrocellulose-coated glass capillaries were first incubated with Ti I-II (5 μM) and were then blocked (5 mg/ml BSA). Myosin (0.5 mg/ml) or HMM (0.6 mg/ml) was then added, followed by washing. Bound protein was solubilized and subjected to electrophoresis. Lanes 1 and 5 were loaded with only myosin and HMM, respectively. Lanes 2 and 6 were blocked and then loaded with myosin and HMM, respectively. Lanes 3 and 4 were coated with Ti I-II, blocked, and then incubated with myosin in a buffer with an ionic strength of 340 mM followed by either washing with this buffer (lane 3) or washing with in vitro motility assay buffer (lane 4). Lane 7 was coated with Ti I-II, blocked, loaded with HMM, and then washed with in vitro motility buffer. See text for additional details. (The band in lane 1 with mobility similar to that of BSA may be a contaminant.)

1993). This finding is consistent with the idea of interaction between titin and F-actin. Titin-actin interaction might thus be a universal property that occurs both in vitro and in vivo under a wide range of conditions.

How many of the ~300 motifs of the titin molecule interact with actin filaments remains to be established. It seems likely that some of the motifs that are found at the edge of the A-band and in the I-band can bind F-actin because antibodies against Ti I-II label these regions of the sarcomere (Jin, 1995; Granzier et al., in preparation). Additionally, it cannot be discounted that other A-band and I-band motifs that are not recognized by anti-Ti I-II antibodies nevertheless have binding properties similar to those of the Ti I-II fragment. It is likely that titin binds to thick filaments in the A-band (Wang et al., 1984; Fürst et al., 1988; Whiting et al., 1989; Trombitás et al., 1991), but this does not exclude the possibility that A-band titin contains sufficient lateral freedom to allow it to interact also with actin. Because I-band titin elongates when muscle is slowly stretched (Wang et al., 1984; Fürst et al., 1988), titin-actin interaction in the I-band would have to be rapidly reversible, as we found for Ti I-II-actin interaction. Rapidly reversible interaction allows both I-band titin to behave elastically and actin filaments to slide unobstructed in and out of the A-band. This type of titin-actin interaction could manifest itself, however, when sliding occurs very rapidly and may explain the finding of de Tombe and ter Keurs (1992) that the unloaded velocity of sarcomere shortening in rat myocardium may be limited by titin.

Titin-actin interaction in the I-band could in principle also affect passive tension developed by striated muscle. This proposal is consistent with the finding that after actin removal from skeletal muscle fibers with gelsolin, the sarcomere slack length is shorter and the passive tension-sarcomere length relation is steeper (Granzier and Wang, 1993a). In unstretched sarcomeres, titin filaments are not straight but folded, and the passive tension level of stretched sarcomeres is determined at moderate degrees of stretch by unfolding of the titin filament and at higher degrees of stretch by unfolding of the different titin motifs along the titin molecule (Wang et al., 1991; Soteriou et al., 1993a; Erickson, 1994). Titin-actin interaction may thus modulate the conformation of titin and thereby influence passive tension.

In summary, we have shown that titin fragments inhibit actin sliding in the in vitro motility assay. It is now worth investigating the physiological relevance of this in the more complex in vivo system.

This work was supported by a grant-in-aid of the American Heart Association (Washington State Affiliate) and a Whitaker Foundation grant for biomedical research to Henk L. Granzier; and by a grant-in-aid from the Heart and Stroke Foundation of Alberta to Jian-Ping Jin. Jian-Ping Jin is a recipient of a research scholarship from the Heart and Stroke Foundation of Canada and a developmental grant from the Medical Research Council of Canada. We express our gratitude to Drs. Miklós Kellermayer and Tom Irving for critical reading of various drafts of the manuscript, and to Bronislava Stockman and Mary Resek for superb technical assistance.

REFERENCES

de Tombe, P., and H. ter Keurs. 1992. An internal viscous element limits unloaded velocity of sarcomere shortening in rat myocardium. *J. Physiol.* 454:619–642.

Erickson, H. 1994. Reversible unfolding of fibronectin type III and immunoglobulin domains provides the structural basis for stretch and elasticity of titin and fibronectin. *Proc. Natl. Acad. Sci. USA.* 91:10114–10118.

Finer, J., R. Simmons, and J. Spudich. 1994. Single myosin molecule mechanics: piconewton forces and nanometer steps. *Nature.* 368: 113–119.

Fritz, J., J. Wolff, and M. Greaser. 1993. Characterization of a partial cDNA clone encoding porcine skeletal muscle titin: comparison with rabbit and mouse skeletal muscle titin sequences. *Comp. Biochem. Physiol.* 105B:357–360.

Fulton, A., and W. Isaacs. 1991. Titin, a huge, elastic sarcomeric protein with a probable role in morphogenesis. *Bioessays.* 13:157–161.

Funatsu, T., E. Kono, H. Higuchi, S. Kimura, S. Ishiwata, T. Yoshioka, K. Maruyama, and S. Tsukita. 1993. Elastic filaments in situ in cardiac muscle: deep-etch replica analysis in combination with selective removal of actin and myosin filaments. *J. Cell Biol.* 120:711–724.

Fürst, D., M. Osborn, M. Nave, and K. Weber. 1988. The organization of titin filaments in the half-sarcomere revealed by monoclonal antibodies in immunoelectron microscopy: a map of ten nonrepetitive epitopes starting at the Z-line extends close to the M-line. *J. Cell Biol.* 106: 1563–1572.

Granzier, H. L. M., and T. Irving. 1995. Passive tension in cardiac muscle: the contribution of collagen, titin, microtubules and intermediate filaments. *Biophys. J.* 68:1027–1044.

Granzier, H. L. M., and K. Wang. 1993a. Passive tension and stiffness of vertebrate skeletal muscle and insect flight muscle: the contribution of weak crossbridges and elastic filaments. *Biophys. J.* 65:2141–2159.

Granzier, H. L. M., and K. Wang. 1993b. Gel electrophoresis of giant proteins: solubilization and silver staining of titin and nebulin from single muscle fiber segments. *Electrophoresis.* 14:56–64.

Granzier, H. L. M., and K. Wang. 1993c. Interplay between passive tension and strong and weak cross-bridges in insect asynchronous flight muscle: a functional dissection by gelsolin mediated thin filament removal. *J. Gen. Physiol.* 101:235–270.

Haeberle, J., K. Trybus, M. Hemric, and D. Warshaw. 1992. The effects of smooth muscle caldesmon on actin filament motility. *J. Biol. Chem.* 267:23001–23006.

Higuchi, H., 1992. Changes in contractile properties with selective digestion of connectin (titin) in skinned fibers of frog skeletal muscle. *J. Biochem.* 111:291–295.

Higuchi, H., T. Suzuli, S. Kimura, S. Yoshioka, K. Maruyama, and Y. Umazuma. 1992. Localization and elasticity of connectin (titin) filaments in skinned frog muscle fibers subjected to partial depolymerization of thick filaments. *J. Muscle Res. Cell Motil.* 13:285–294.

Homsher, E., F. Wang, and J. Sellers. 1992. Factors affecting movement of F-actin filaments propelled by skeletal muscle heavy meromyosin. *Am. J. Physiol.* 262:C714–C723.

Horowits, R., E. S. Kempner, M. E. Bisher, and R. Podolsky. 1986. A physiological role for titin and nebulin in skeletal muscle. *Nature.* 323:160–164.

Jin, J.-P. 1995. Cloned rat cardiac titin class I and class II motifs: expression, purification, characterization, and interaction with F-actin. *J. Biol. Chem.* 270:6908–6916.

Kimura, S., K. Maruyama, and Y. Huang. 1984. Interactions of muscle β-connectin with myosin, actin, and actomyosin at low ionic strength. *J. Biochem.* 96:499–506.

Kishino, A., and T. Yanagida. 1988. Force measurements by micromanipulation of a single actin filament by glass needles. *Nature.* 334:74–76.

Koretz, J., T. Irving, T., and K. Wang. 1993. Filamentous aggregates of native titin and binding of C-protein and AMP-deaminase. *Arch. Biochem. Biophys.* 304:305–309.

Kron, S., Y. Toyoshima, T. Uyeda, and J. Spudich. 1991. Assays for actin sliding movement over myosin coated surface. *Methods Enzymol.* 196: 399–416.

Labeit, S., D. Barlow, M. Gautel, T. Gibson, C. Hsieh, U. Francke, K. Leonard, J. Wardale, A. Whiting, and J. Trinick. 1990. A regular pattern of two types of 100-residue motif in the sequence of titin. *Nature.* 345:273–276.

Labeit, S., M. Gautel, A. Lackey, and J. Trinick. 1992. Towards a molecular understanding of titin. *EMBO J.* 11:1711–1716.

Margossian, S., and S. Lowey. 1982. Preparation of myosin and its subfragments from rabbit skeletal muscle. *Methods Enzymol.* 85:55–72.

Maruyama, K. 1986. Connectin an elastic filamentous protein of striated muscle. *Int. Rev. Cytol.* 104:81–114.

Maruyama, K. 1994. Connectin, an elastic protein of striated muscle. *Biophys. Chem.* 50:73–85.

Maruyama, K., D. Hu, T. Suzuki, and S. Kimura. 1987. Binding of actin filaments to connectin. *J. Biochem.* 101:1339–1346.

Maruyama, K., T. Endo, H. Kume, Y. Kawamura, N. Kanzawa, Y. Nakauchi, S. Kimura, and K. Maruyama. 1993. *Biochem. Biophys. Res. Commun.* 194:1288.

Pan, K., S. Damodaran, and M. Greaser. 1994. Isolation and characterization of titin T1 from bovine cardiac muscle. *Biochemistry.* 33: 8255–8261.

Politou, A., M. Gautel, M. Pfuhl, S. Labeit, and A. Pastore. 1994. Immunoglobulin-type domains of titin: same fold different stability? *Biochemistry.* 33:4730–4737.

Sebestyén, M., J. Wolff, and M. Greaser. 1995. Characterization of a novel 5.4 kb cDNA fragment coding for the N-terminal region of rabbit cardiac titin. *Biophys. J.* 68:65*a*. (Abstr.)

Sellers, J., G. Cuda, F. Wang, and E. Homsher. 1993. Myosin-specific adaptations of the motility assay. *Methods Cell Biol.* 39:24–48.

Soteriou, A., A. Clarke, S. Martin, and J. Trinick. 1993a. Titin folding energy and elasticity. *Proc. R. Soc. London B Biol. Sci.* 254:83–86.

Soteriou, A., M. Gamage, and J. Trinick. 1993b. A survey of interactions made by the giant protein titin. *J. Cell Sci.* 104:119–123.

Toyoshima, Y. 1993. How are myosin fragments bound to nitrocellulose film? *In* Mechanism of myofilament sliding in muscle contraction. H. Sugi and G. Pollack, editors. Plenum Press, New York. 259–265.

Trinick, J. 1991. Elastic filaments and giant proteins in muscle. *Curr. Opin. Cell Biol.* 3:112–118.

Trombitás, K., and G. Pollack. 1993. Elastic properties of the titin filament in the Z-line region of vertebrate striated muscle. *J. Muscle Res. Cell Motil.* 14:416–422.

Trombitás, K., P. Baatsen, M. Kellermayer, and G. Pollack. 1991. Nature and origin of gap filaments in striated muscle. *J. Cell Sci.* 100:809–814.

Wang, K. 1985. Sarcomere-associated cytoskeletal lattices in striated muscle. *Cell Muscle Motil.* 6:315–369.

Wang, K., R. McCarter, J. Wright, B. Jennate, and R. Ramirez-Mitchell. 1991. Regulation of skeletal muscle stiffness and elasticity by titin isoforms. *Proc. Natl. Acad. Sci. USA.* 88:7101–7109.

Wang, K., R. McCarter, J. Wright, B. Jennate, and R. Ramirez-Mitchell. 1993. Viscoelasticity of the sarcomere matrix of skeletal muscles: the titin-myosin composite filament is a dual-range molecular spring. *Biophys. J.* 64:1161–1177.

Wang, K., J. Wright, and R. Ramirez-Mitchell. 1984. Architecture of the titin/nebulin containing cytoskeletal lattice of the striated muscle sarcomere: evidence of elastic and inelastic domains of the bipolar filaments. *J. Cell Biol.* 99(4, Pt 2): 435*a*. (Abstr.)

Whiting, A., J. Wardale, and J. Trinick. 1989. Does titin regulate the length of muscle thick filaments? *J. Mol. Biol.* 205:163–169.

Yamashita, H., M. Sata, S. Sugiura, S. Momomura, T. Serizawa, and M. Iizuka. 1994. ADP inhibits the sliding velocity of fluorescent actin filaments on cardiac and skeletal myosins. *Circ. Res.* 74:1027–1033.

Yoshioka, T., H. Higuchi, S. Kimura, K. Ohashi, Y. Umazume, and K. Maruyama. 1986. Effects of mild trypsin treatment on the passive tension generation and connectin splitting in stretched skinned fibers from frog skeletal muscle. *Biomed. Res.* 7:181–186.